

Scalar Field Green Functions on Causal Sets

Nomaan X¹, Fay Dowker², and Sumati Surya¹

¹*Raman Research Institute, C.V. Raman Avenue, Sadashivnagar, Bangalore 560 080, India*

²*Blackett Laboratory, Imperial College, London, SW7 2AZ, UK*

We examine the validity and scope of Johnston’s models for scalar field retarded Green functions on causal sets in 2 and 4 dimensions. As in the continuum, the massive Green function can be obtained from the massless one, and hence the key task in causal set theory is to first identify the massless Green function. We propose that the 2-d model provides a Green function for the massive scalar field on causal sets approximated by any topologically trivial 2 dimensional spacetime. We explicitly demonstrate that this is indeed the case in a Riemann normal neighbourhood. In 4-d the model can again be used to provide a Green function for the massive scalar field in a Riemann normal neighbourhood which we compare to Bunch and Parker’s continuum Green function. We find that the same prescription can also be used for deSitter spacetime and the conformally flat patch of anti deSitter spacetime. Our analysis then allows us to suggest a generalisation of Johnston’s model for the Green function for a causal set approximated by 3 dimensional flat spacetime.

1 Introduction

Understanding classical and quantum scalar field propagation on a fixed causal set is an important problem in causal set quantum gravity [1, 2, 3, 4, 5, 6]. Although ignoring back reaction and the quantum dynamics of the causal set background itself means that the treatment of scalar field dynamics will be inconsistent in some way, we can hope to learn something about causal set theory by studying this problem. Recent progress in defining scalar quantum field theory on a causal set puts great importance on the retarded Green function for the field on the causal set. Such a Green function can be used to obtain the Feynman propagator, or equivalently the Wightman function, of a distinguished quantum state on a causal set C , the *Sorkin-Johnston state* [7, 8]. This could have potentially interesting phenomenological consequences [8]. Sorkin’s related construction of a double path integral form of free scalar quantum field theory on a finite casual set is also based on the retarded Green function [9].

Johnston found massive scalar field retarded Green functions, $K_m(x, x')$, for causal sets approximated by $d = 2$ and $d = 4$ Minkowski spacetime [3, 4]. For each case, he used a “hop-stop”

ansatz in which the Green function equals a sum over appropriately chosen causal trajectories between the two arguments of the Green function, with a weight assigned for every hop between the elements of the trajectory and another for every stop at an intervening element. Requiring that the continuum limit of the mean of the causal set Green function over Poisson point process samplings – so-called sprinklings – of the Minkowski spacetime equals the continuum retarded Green function then fixes these weights. Extending the scope of the hop-stop ansatz to a larger class of causal sets would therefore allow us to study causal set quantum field theory further.

We begin by describing Johnston’s model in Section 2 and explain how it can be motivated by a spacetime treatment. We will see that the key is to identify the appropriate retarded Green function for the *massless* field. This then leads to our proposed extensions of the model in Section 3. For $d = 2$ we propose that Johnston’s definition of $K_m(x, x')$ can be used for a minimally coupled massive scalar field on a causal set approximated by any topologically trivial spacetime. The proposal stems from the fact that the massless, minimally coupled scalar field theory is conformally invariant. In $d = 2$, for non minimal coupling – *i.e.* with arbitrary coupling to the Ricci scalar – we show that the Johnston $K_m(x, x')$ is an appropriate retarded Green function in an approximately flat Riemann Normal Neighbourhood, up to corrections. In $d = 4$ we find that it is possible to extend the Minkowski spacetime prescription to an RNN, as well as de Sitter spacetime and the conformally flat patch of anti de Sitter spacetime. In all cases, the comparison with the continuum fixes the hop-stop weights. Our results are *exact* for de Sitter and the globally hyperbolic patch of anti de Sitter spacetime, *i.e.*, the limit of the mean of the massless causal set Green function is the conformally coupled massless Green function. In Section 4 we use this framework to propose a construction of the retarded Green functions on $d = 3$ Minkowski spacetime. Throughout the paper we assume that the spacetimes we are considering are globally hyperbolic.

2 The Model

Consider the massless scalar retarded Green function $G_0(x, x')$ on a globally hyperbolic d dimensional spacetime (M, g) :

$$\square_x G_0(x, x') = -\frac{1}{\sqrt{-g(x')}}\delta(x - x'). \quad (1)$$

We can formally write down the massive retarded Green function, G_m , satisfying

$$(\square_x - m^2)G_m(x, x') = -\frac{1}{\sqrt{-g(x)}}\delta(x - x'), \quad (2)$$

as a formal expansion

$$G_m = G_0 - m^2 G_0 * G_0 + m^4 G_0 * G_0 * G_0 + \dots = \sum_{k=0}^{\infty} (-m^2)^k \underbrace{G_0 * G_0 * \dots * G_0}_{k+1} \quad (3)$$

where

$$(A * B)(x, x') \equiv \int d^d x_1 \sqrt{-g(x_1)} A(x, x_1) B(x_1, x'). \quad (4)$$

Note that if $G_0(x, x')$ is retarded (*i.e.* only nonzero if x' is in the causal past of x) then so is $G_m(x, x')$. Also note that since G_0 is retarded, the convolution integrals are over finite regions of spacetime, subsets of the causal interval between x and x' . This relation can be reexpressed in the compact form

$$G_m = G_0 - m^2 G_0 * G_m. \quad (5)$$

Conversely G_0 can be obtained from G_m via

$$G_0 = \sum_{k=0}^{\infty} (m^2)^k \underbrace{G_m * G_m * \dots * G_m}_{k+1} \quad (6)$$

and

$$G_0 = G_m + m^2 G_m * G_0 = G_m + m^2 G_0 * G_m. \quad (7)$$

Once we have the massless retarded Green function, then, we can write down a formal series for the massive retarded Green function.

Now suppose we have in hand a massless retarded Green function analogue, $K_0(x, x')$, on a causal set which is a sprinkling at density ρ into the d -dimensional spacetime. We can immediately propose a massive retarded Green function $K_m(x, x')$ on that causal set via the replacement

$$\int \sqrt{-g(x)} d^d x \rightarrow \rho^{-1} \sum_{\text{causal set elements}}, \quad (8)$$

leading to

$$K_m = K_0 - \frac{m^2}{\rho} K_0 * K_0 + \frac{m^4}{\rho^2} K_0 * K_0 * K_0 + \dots = \sum_{k=0}^{\infty} \left(-\frac{m^2}{\rho} \right)^k \underbrace{K_0 * K_0 * \dots * K_0}_{k+1} \quad (9)$$

where now the convolutions have become finite sums over causal set elements in the finite order interval between x and x' and the series terminates and is well-defined for each pair x and x' .

We will now show that Johnston's hop-stop models for the massive retarded Green functions on causal sets approximated by 2 and 4 dimensional Minkowski space are based on natural causal set analogues of the massless Green functions .

2.1 $d = 2$ Minkowski spacetime

The massless retarded Green function in $d = 2$ Minkowski spacetime \mathbb{M}^2 is

$$G_0^{(2)}(x, x') = \frac{1}{2}\theta(x_0 - x'_0)\theta(\tau^2(x, x')) \quad (10)$$

where $\tau(x, x')$ is defined by

$$\begin{aligned} \tau(x, x') &= \sqrt{(x_0 - x'_0)^2 - (x_1 - x'_1)^2} \quad \text{when } (x_0 - x'_0)^2 \geq (x_1 - x'_1)^2 \\ \text{and} \\ \tau(x, x') &= i\sqrt{-(x_0 - x'_0)^2 + (x_1 - x'_1)^2} \quad \text{when } (x_0 - x'_0)^2 < (x_1 - x'_1)^2. \end{aligned} \quad (11)$$

θ is the Heaviside step function.

Now consider, on a causal set, the *causal matrix*

$$C_0(x, x') \equiv \begin{cases} 1 & \text{if } x' \prec x \\ 0 & \text{otherwise} \end{cases} \quad (12)$$

for all elements x and x' of the causal set, where by \prec we mean causal precedence. The Poisson point process of sprinkling at density ρ in 2 dimensional Minkowski spacetime gives rise to a random variable, $\mathbf{C}_0(x, x')$ for every two points, x and x' , of Minkowski spacetime via the addition of x and x' to the sprinkled causal set and the evaluation of $C_0(x, x')$ on that causal set. Actually, in this case, the random variable takes the same value – the expected value – in each realisation. It was observed in [2] that this value is

$$\langle \mathbf{C}_0(x, x') \rangle = 2G_0^{(2)}(x, x'). \quad (13)$$

This leads to the proposal for a massless retarded Green function, $K_0^{(2)}(x, x')$, on a $d = 2$ flat sprinkled causal set:

$$K_0^{(2)}(x, x') \equiv \frac{1}{2}C_0(x, x'). \quad (14)$$

We define a massive Green function $K_m^{(2)}(x, x')$ on C using this $K_0^{(2)}(x, x')$ and (9).

Let us define a *k-chain between x' and x* in a causal set C as a totally ordered subset of C , $\{x_1, x_2, \dots, x_k\}$ such that $x' \prec x_1 \prec x_2 \prec \dots \prec x_{k-1} \prec x_k \prec x$. For $k \geq 1$, define $C_k(x, x')$ to be the number of k -chains between x and x' when $x' \prec x$ and zero when $x' \not\prec x$. The C_k 's are powers of the causal matrix:

$$C_k(x, x') = \underbrace{C_0 * C_0 * \dots * C_0}_{k+1}(x, x'). \quad (15)$$

This then gives

$$K_m^{(2)}(x, x') = \sum_{k=0}^{\infty} \left(-\frac{m^2}{\rho}\right)^k \left(\frac{1}{2}\right)^{k+1} C_k(x, x'), \quad (16)$$

where the sum is written as an infinite sum but terminates for each pair x and x' .

For each two points x and x' of \mathbb{M}^2 and each k the random variable $\mathbf{C}_k(x, x')$ is $C_k(x, x')$ evaluated on a sprinkled causal set including x and x' , and hence we have the random variable $\mathbf{K}_m^{(2)}(x, x')$:

$$\mathbf{K}_m^{(2)}(x, x') \equiv \sum_{k=0}^{\infty} \left(-\frac{m^2}{\rho} \right)^k \left(\frac{1}{2} \right)^{k+1} \mathbf{C}_k(x, x'). \quad (17)$$

Its mean – for any sprinkling density – is equal to the continuum Green function since

$$\langle \mathbf{C}_k(x, x') \rangle = \rho^k \underbrace{\langle \mathbf{C}_0 * \dots * \mathbf{C}_0 \rangle}_{k+1}(x, x') \quad (18)$$

and so

$$\langle \mathbf{K}_m^{(2)}(x, x') \rangle = \sum_{k=0}^{\infty} \left(-\frac{m^2}{\rho} \right)^k \left(\frac{1}{2} \right)^{k+1} \langle \mathbf{C}_k(x, x') \rangle \quad (19)$$

$$= \sum_{k=0}^{\infty} (-m^2)^k \underbrace{G_0^{(2)} * G_0^{(2)} * \dots * G_0^{(2)}}_{k+1}(x, x') \quad (20)$$

$$= G_m^{(2)}(x, x'). \quad (21)$$

In [3] $K_m^{(2)}(x, x')$ was expressed in terms of the hop and stop weights, a and b respectively:

$$K_m^{(2)}(x, x') = \sum_{k=0}^{\infty} a^{k+1} b^k C_k(x, x'). \quad (22)$$

This form was described by Johnston using a particle language as a sum over all chains between x and x' : for each k -chain the hop between two successive elements is assigned the weight a and the stop at each intervening element between x and x' is assigned the weight b . Now we see that the weight $a = \frac{1}{2}$ is associated to each factor of $K_0^{(2)}$ – from the relationship between $K_0^{(2)}$ and the causal matrix – and the weight $b = -\frac{m^2}{\rho}$ to each convolution. In [3] a momentum space calculation was used to find b , but as we have just seen the spacetime formulation is sufficient to read off the value.

2.2 $d = 4$ Minkowski spacetime

In $d = 4$ Minkowski spacetime, \mathbb{M}^4 , the retarded Green function for the massless field only has support on the light cone:

$$G_0^{(4)}(x, x') = \frac{1}{2\pi} \theta(x_0 - x'_0) \delta(\tau^2(x, x')), \quad (23)$$

where

$$\tau(x, x') = \sqrt{(x_0 - x'_0)^2 - (x_1 - x'_1)^2 - (x_2 - x'_2)^2 - (x_3 - x'_3)^2} \quad \text{when} \\ (x_0 - x'_0)^2 \geq (x_1 - x'_1)^2 + \dots + (x_3 - x'_3)^2$$

and

$$\tau(x, x') = i \sqrt{-(x_0 - x'_0)^2 + (x_1 - x'_1)^2 + (x_2 - x'_2)^2 + (x_3 - x'_3)^2} \quad \text{when} \\ (x_0 - x'_0)^2 < (x_1 - x'_1)^2 + \dots + (x_3 - x'_3)^2. \quad (24)$$

The causal set analogue is proportional to the *link matrix*

$$L_0(x, x') := \begin{cases} 1 & \text{if } x' \prec x \text{ and } |[x, x']| = 0 \\ 0 & \text{otherwise} \end{cases} \quad (25)$$

where the *exclusive interval* is defined by $[x, x'] \equiv \{z \in C \mid x' \prec z \prec x\}$. When $x' \prec x$ and $|[x, x']| = 0$ this relation is called a *link*. The expectation value of the corresponding random variable $\mathbf{L}_0(x, x')$ in a Poisson sprinkling of density ρ is

$$\langle \mathbf{L}_0(x, x') \rangle = \theta(x_0 - x'_0) \theta(\tau^2(x, x')) \exp(-\rho V(x, x')), \quad (26)$$

where $V(x, x')$ is the volume of the spacetime interval $J^-(x) \cap J^+(x')$. Here $J^+(x)$ and $J^-(x)$ denote ¹ the causal future and past of x , respectively. In \mathbb{M}^4 , $V(x, x') = \frac{\pi}{24} \tau^4(x, x')$, so that

$$\lim_{\rho \rightarrow \infty} \sqrt{\frac{\rho}{6}} \langle \mathbf{L}_0(x, x') \rangle = 2 \theta(x_0 - x'_0) \theta(\tau^2) \delta(\tau^2) \quad (27)$$

$$= \theta(x_0 - x'_0) \delta(\tau^2) \quad (28)$$

$$= 2\pi G_0^{(4)}(x, x'). \quad (29)$$

This therefore suggests that we take the massless Green function on a flat 4-d causal set to be

$$K_0^{(4)}(x, x') = \frac{1}{2\pi} \sqrt{\frac{\rho}{6}} L_0(x, x'). \quad (30)$$

The relationship with the continuum Green function is not so direct as in $d = 2$ since here it is only in the continuum limit as $\rho \rightarrow \infty$ that the mean of $K_0^{(4)}$ over sprinklings equals the continuum $G_0^{(4)}$. We use this $K_0^{(4)}$ to construct a massive Green function $K_m^{(4)}(x, x')$ via (9) as before.

Let a *k-path between x' and x* in a causal set C be a *k-chain* between x' and x , $x' \prec x_1 \prec x_2 \prec \dots \prec x_{k-1} \prec x_k \prec x$, in which all these relations are links. For $k \geq 1$, define $L_k(x, x')$ to be the number of *k-paths* between x' and x when $x' \prec x$ and zero when $x' \not\prec x$. The L_k 's are powers of the link matrix:

$$L_k(x, x') = \underbrace{L_0 * L_0 * \dots * L_0}_{k+1}(x, x'). \quad (31)$$

¹see Wald for example

This gives

$$K_m^{(4)}(x, x') = \sum_{k=0}^{\infty} \left(-\frac{m^2}{\rho}\right)^k \left(\frac{1}{2\pi} \sqrt{\frac{\rho}{6}}\right)^{k+1} L_k(x, x'), \quad (32)$$

where the sum terminates for each pair x and x' .

For each two points x and x' of \mathbb{M}^2 and each k , the random variable $\mathbf{L}_k(x, x')$ is $L_k(x, x')$ evaluated on a sprinkled causal set including x and x' , and hence we have the random variable $\mathbf{K}_m^{(4)}(x, x')$:

$$\mathbf{K}_m^{(4)}(x, x') \equiv \sum_{k=0}^{\infty} \left(-\frac{m^2}{\rho}\right)^k \left(\frac{1}{2\pi} \sqrt{\frac{\rho}{6}}\right)^{k+1} \mathbf{L}_k(x, x'). \quad (33)$$

The limit as $\rho \rightarrow \infty$ of its mean is equal to the series for the continuum Green function since

$$\langle \mathbf{L}_k(x, x') \rangle = \rho^k \underbrace{(\langle \mathbf{L}_0 \rangle * \dots * \langle \mathbf{L}_0 \rangle)}_{k+1}(x, x') \quad (34)$$

and so

$$\lim_{\rho \rightarrow \infty} \langle \mathbf{K}_m^{(4)}(x, x') \rangle = \lim_{\rho \rightarrow \infty} \sum_{k=0}^{\infty} \left(-\frac{m^2}{\rho}\right)^k \left(\frac{1}{2\pi} \sqrt{\frac{\rho}{6}}\right)^{k+1} \langle \mathbf{L}_k(x, x') \rangle \quad (35)$$

$$= \lim_{\rho \rightarrow \infty} \sum_{k=0}^{\infty} (-m^2)^k \left(\frac{1}{2\pi} \sqrt{\frac{\rho}{6}}\right)^{k+1} \underbrace{\langle \mathbf{L}_0 \rangle * \dots * \langle \mathbf{L}_0 \rangle}_{k+1}(x, x') \quad (36)$$

$$= \sum_{k=0}^{\infty} (-m^2)^k \underbrace{G_0^{(4)} * G_0^{(4)} * \dots * G_0^{(4)}}_{k+1}(x, x') \quad (37)$$

$$= G_m^{(4)}(x, x'). \quad (38)$$

Johnston interpreted (30) as a sum over paths between x and x' . The hop-stop weights can be read off from Eqn (33) as $a = \frac{1}{2\pi} \sqrt{\frac{\rho}{6}}$ and $b = -\frac{m^2}{\rho}$, respectively.

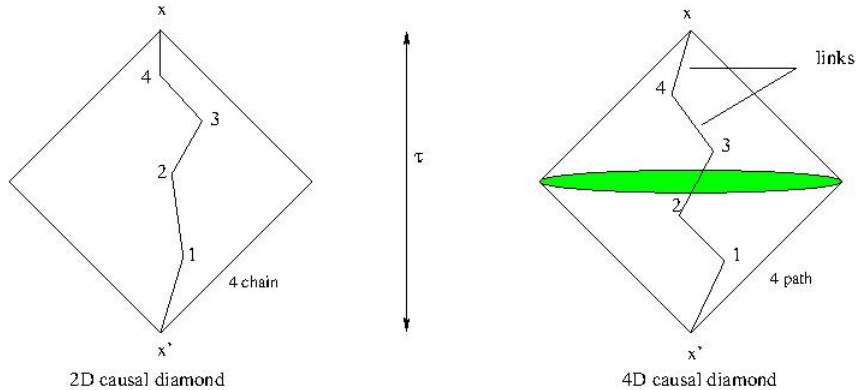


Figure 1: The causal trajectories in $d = 2$ and 4 dimensions.

3 Generalisations

The key to the above construction of a massive Green function is knowing the massless one. We can repeat it if we can find the massless retarded Green function for causal sets sprinkled into more general curved spacetimes.

Consider the more general scalar theory with nonminimal coupling with Green function $G_{m,\xi}(x, x')$ which satisfies

$$(\square_g - m^2 - \xi R)G_{m,\xi}(x, x') = \frac{1}{\sqrt{-g(x)}}\delta(x - x'). \quad (39)$$

$G_{m,\xi}(x, x')$ can be obtained from $G_{0,\xi}(x, x')$ using the same series expansion Eqn(3):

$$G_{m,\xi} = \sum_{k=0}^{\infty} (-m^2)^k \underbrace{G_{0,\xi} * G_{0,\xi} * \dots * G_{0,\xi}}_{k+1}. \quad (40)$$

In the special case when the spacetime has constant scalar curvature R , then the ξR term just modifies the mass and $G_{m,\xi}(x, x')$ can be obtained from the minimally coupled massless Green function $G_{0,0}(x, x')$ using a series expansion Eqn(3) with m^2 replaced by $m^2 + \xi R$. In general, for constant R , we can relate the two Green functions

$$G_{m',\xi'} = \sum_{k=0}^{\infty} (-m'^2 - \xi' R + m^2 + \xi R)^k \underbrace{G_{m,\xi} * G_{m,\xi} * \dots * G_{m,\xi}}_{k+1}, \quad (41)$$

for any $(m, \xi), (m', \xi')$.

We seek analogous massive scalar Green functions, $K_{m,\xi}(x, x')$, for causal sets sprinkled into nonflat spacetimes. We will see that this is possible in special cases.

3.1 $d = 2$

Every $d = 2$ spacetime is locally conformally flat. The conformal coupling in $d = 2$ is $\xi = 0$, *i.e.* conformal coupling is minimal coupling. If the spacetime is topologically trivial and consists of one patch covered by conformally flat coordinates, then the minimally coupled massless Green function equals the flat spacetime Green function (10).

Therefore, we propose that on causal sets sprinkled into such $d = 2$ spacetimes, the massless minimally coupled causal set Green function, $K_{0,0}^{(2)}(x, x')$, is the flat one given by Eqn (14) and therefore that $K_{m,0}^{(2)}(x, x')$ is the flat one given by Eqn (16):

$$K_{m,0}^{(2)}(x, x') = \sum_{k=0}^{\infty} \left(-\frac{m^2}{\rho}\right)^k \left(\frac{1}{2}\right)^{k+1} C_k(x, x'), \quad (42)$$

The argument that the mean over sprinklings of the corresponding random variable will be the correct continuum Green function proceeds exactly as in the flat case: (16)–(21). However it is formal and we will provide more concrete evidence. We will verify directly that this $K_{m,0}^{(2)}$ does have the correct mean value over sprinklings in a Riemann Normal Neighbourhood (RNN).

In our calculation below as well as in Section 3.2.1, the RNN should be seen as providing an intermediate scale at which the continuum description is still valid, and which is therefore much larger than the discreteness scale. The reason to use the RNN is simply that the calculations can be done explicitly to leading order both in the causal set as well as the continuum.

3.1.1 RNN in $d = 2$

Consider the RNN (O, g) with Riemann normal coordinates with origin x' . The metric at $x \in O$ can be expanded to first order about x' in these coordinates as

$$g_{ab}(x) = \eta_{ab} + \frac{1}{2!} \partial_c \partial_d g_{ab}(x') x^c x^d + \mathcal{O}(x^3). \quad (43)$$

where η_{ab} is the metric of Minkowski spacetime in inertial coordinates and $\partial_c g_{ab}(x') = 0$. We assume that the RNN is approximately flat, *i.e.* $|R\tau^2(x, x')| \ll 1$, and work in an approximation where we drop terms involving derivatives of the curvature or quadratic and higher powers of the curvature.

The d dimensional momentum space Green function in a RNN has been calculated by Bunch and Parker [10]. To leading order the density

$$\mathbb{G}_{m,\xi}(x, x') \equiv (-g(x))^{\frac{1}{4}} G_{m,\xi}(x, x') \quad (44)$$

satisfies the equation

$$(\square_\eta - (m^2 + (\xi - \frac{1}{6})R(x')))\mathbb{G}_{m,\xi}(x, x') \approx -\delta(x - x'), \quad (45)$$

where $\square_\eta = \eta^{ab} \nabla_a \nabla_b$ and acts on the x argument. This has the momentum space solution

$$\mathbb{G}_{m,\xi}(p) \approx \frac{1}{p^2 + m^2} - (\xi - \frac{1}{6})R(x') \frac{1}{(p^2 + m^2)^2}. \quad (46)$$

This solution was obtained iteratively using the expansion

$$\mathbb{G}_{m,\xi}(p) = \mathbb{G}_{m,\xi,0}(p) + \mathbb{G}_{m,\xi,1}(p) + \mathbb{G}_{m,\xi,2}(p) + \dots \quad (47)$$

where $\mathbb{G}_{m,\xi,0}(p) = (k^2 + m^2)^{-1}$ is the flat spacetime Green function which is independent of ξ . This expansion is valid when the Compton wavelength of the particle is much smaller than the

curvature scale, i.e., $m^2 \gg \xi R$, a physically reasonable assumption. The spacetime function can then be expressed as

$$\mathbb{G}_{m,\xi}(x, x') \approx G_m^F(x, x') + \frac{1}{2m}(\xi - \frac{1}{6})R(x') \partial_m G_m^F(x, x'), \quad (48)$$

where $G_m^F(x, x')$ is the massive minimally coupled Green function in \mathbb{M}^d . The Green function is then

$$G_{m,\xi}(x, x') \approx \left(1 + \frac{1}{12}R_{ab}(x')x^a x^b\right) G_m^F(x, x') + \frac{1}{2m}(\xi - \frac{1}{6})R(x') \partial_m G_m^F(x, x'). \quad (49)$$

Now we specialise to $d = 2$. Using the $d = 2$ Minkowski spacetime solution for the massive retarded solution

$$\frac{1}{2}\theta(x_0)\theta(\tau^2)J_0(m\tau), \quad (50)$$

where $\tau = \tau(x, x')$ (11), the retarded massive Green function in (O, g) is given by

$$G_{m,\xi}^{(2)}(x, x') \approx \theta(x_0)\theta(\tau^2) \left[\frac{1}{2}J_0(m\tau) + \frac{R(x')\tau^2}{48}J_2(m\tau) - \frac{\xi R(x')\tau}{4m}J_1(m\tau) \right]. \quad (51)$$

Let us define

$$\mathcal{K}^{(2)}(a, b)(x, x') \equiv \sum_{k=0}^{\infty} a^{k+1} b^k C_k(x, x') \quad (52)$$

for arbitrary weights a and b . We want to show that the corresponding random variable for sprinklings into a RNN has the correct mean value, (51) when a and b take their flat space values $a = \frac{1}{2}$ and $b = -\frac{m^2}{\rho}$.

We can calculate $\langle \mathcal{K}^{(2)}(a, b)(x, x') \rangle$ starting from Eqn (52) if we know $\langle \mathbf{C}_k(x, x') \rangle$ in a small causal diamond. This was calculated, to first order in curvature, in [11] for arbitrary $d \geq 2$. In $d = 2$ the expression is

$$\langle \mathbf{C}_k(x, x') \rangle \approx \langle \mathbf{C}_k(x, x') \rangle_{\eta} \left(1 - \frac{R(x')\tau^2}{24} \frac{k}{k+1} \right) \quad (53)$$

where $\langle \mathbf{C}_k(x, x') \rangle_{\eta} = \theta(x_0)\theta(\tau^2) \frac{1}{\Gamma(k+1)^2} \left(\frac{\rho\tau^2}{2} \right)^k$ is the mean in flat space. Using the series expansion of the Bessel functions we see that

$$\begin{aligned} \langle \mathcal{K}^{(2)}(a, b) \rangle &\approx \theta(x_0)\theta(\tau^2) \sum_{k=0}^{\infty} a^{k+1} b^k \left(\frac{\rho\tau^2}{2} \right)^k \frac{1}{(\Gamma(k+1))^2} \left(1 - \frac{R(x')\tau^2}{24} \frac{k}{k+1} \right) \\ &\approx \theta(x_0)\theta(\tau^2) \left[a I_0(\tau\sqrt{2ab\rho}) - \frac{aR(x')\tau^2}{24} I_2(\tau\sqrt{2ab\rho}) \right]. \end{aligned} \quad (54)$$

If we set $a = \frac{1}{2}$, $b = -\frac{m^2}{\rho}$ we find

$$\langle \mathcal{K}^{(2)}\left(\frac{1}{2}, -\frac{m^2}{\rho}\right)(x, x') \rangle \approx \theta(x_0)\theta(\tau^2) \left[\frac{1}{2}J_0(m\tau) + \frac{R(x')\tau^2}{48}J_2(m\tau) \right], \quad (55)$$

which matches Eqn (51) for $\xi = 0$.

We further note that in the RNN since $R(x') \approx R$, a constant to this order of approximation, we can use the observation above that ξR can be treated as a contribution to the mass. Putting $a = \frac{1}{2}$ and $b = -\frac{(m^2 + \xi R)}{\rho}$ in (54) and using $m^2 \gg \xi R$, we obtain

$$\begin{aligned} & \theta(x_0)\theta(\tau^2) \left[\frac{1}{2} J_0(\tau\sqrt{m^2 + \xi R}) + \frac{R\tau^2}{48} J_2(\tau\sqrt{m^2 + \xi R}) \right] \\ & \approx \theta(x_0)\theta(\tau^2) \left[\frac{1}{2} \sum_{n=0}^{\infty} \frac{(-1)^n}{(n!)^2} \left(\frac{\tau}{2}\right)^{2n} (m^2 + \xi R)^n + \frac{R\tau^2}{48} J_2(m\tau) \right] \\ & \approx \theta(x_0)\theta(\tau^2) \left[\frac{1}{2} J_0(m\tau) + \frac{R\tau^2}{48} J_2(m\tau) - \frac{\xi R\tau}{4m} J_1(m\tau) \right] \end{aligned} \quad (56)$$

which agrees with Eqn (51). Thus, for a causal set sprinkled into an approximately flat causal diamond in $d = 2$, Eqn (52) with $a = \frac{1}{2}$ and $b = -\frac{(m^2 + \xi R(x'))}{\rho}$ is approximately the “right” massive causal set Green function for general coupling ξ .

3.2 $d = 4$

3.2.1 RNN in $d = 4$

The approximate continuum retarded Green function in the RNN in $d = 4$ simplifies to

$$G_{m,\xi}^{(4)}(x, x') \approx \theta(x_0) \left[\left(\frac{1}{2\pi} \delta(\tau^2) - \theta(\tau^2) \frac{m}{4\pi\tau} J_1(m\tau) \right) \left(1 + \frac{1}{12} R_{ab}(x') x^a x^b \right) \right] \quad (57)$$

$$- \theta(x_0)\theta(\tau^2) \left(\xi - \frac{1}{6} \right) \frac{R(x')}{8\pi} J_0(m\tau), \quad (58)$$

which reduces to the massless Green function

$$G_{0,\xi}^{(4)}(x, x') \approx \frac{1}{2\pi} \theta(x_0) \delta(\tau^2) \left(1 + \frac{1}{12} R_{ab}(x') x^a x^b \right) - \theta(x_0)\theta(\tau^2) \left(\xi - \frac{1}{6} \right) \frac{R(x')}{8\pi}. \quad (59)$$

Even this simplified expression is formidable to mimic in the causal set since not only does it require the discrete scalar curvature [12] but also the *components* of the Ricci curvature for which no expression is known. However, for conformal coupling $\xi = \frac{1}{6}$ and Einstein spaces with Ricci curvature $R_{ab} \propto g_{ab}$, (59) reduces to the Minkowski spacetime form (23). Indeed, we only require that $R_{ab}(x') \propto g_{ab}(x')$ upto the order we are considering. This suggests that the flat spacetime massless causal set Green function (30) may give the right continuum Green function. Since R is approximately constant in the RNN (and exactly constant in an Einstein space) we can use the series in powers of the massless Green function to propose the massive one for arbitrary ξ .

For the massless field let us calculate the mean of the link matrix, given by (26). The spacetime volume in the RNN has corrections to the Minkowski spacetime volume $V_\eta(x, x')$ [13, 14, 15] which in $d = 4$ are

$$V(x, x') \approx V_\eta(x, x') \left(1 - \frac{1}{180} R(x') \tau^2 + \frac{1}{30} R_{ab}(x') x^a x^b \right). \quad (60)$$

To leading order then

$$\langle \mathbf{L}_0(x, x') \rangle \approx \theta(x_0) \theta(\tau^2) e^{-\rho V_\eta(x, x')} \left(1 + \frac{\rho V_\eta(x, x')}{180} R(x') \tau^2 - \frac{\rho V_\eta(x, x')}{30} R_{ab}(x') x^a x^b \right). \quad (61)$$

Since $V_\eta(x, x') = \frac{\pi}{24} \tau^4(x, x')$, $\sqrt{\rho} \langle \mathbf{L}_0(x, x') \rangle$ contains terms of the form

$$h_n(\rho, \tau) \equiv \sqrt{\rho} (c\rho\tau^4)^n \exp(-c\rho\tau^4), \quad (62)$$

with $n = 0, 1$. As shown in Appendix A

$$\lim_{\rho \rightarrow \infty} h_n(\rho, \tau) = \frac{\Gamma(n + 1/2)}{2\sqrt{c}} \delta(\tau^2). \quad (63)$$

Using this, we find that

$$\lim_{\rho \rightarrow \infty} \frac{\sqrt{\rho}}{2\pi\sqrt{6}} \langle \mathbf{L}_0(x, x') \rangle \approx \frac{1}{2\pi} \theta(x_0) \delta(\tau^2) \left(1 + \frac{R(x') \tau^2}{360} - \frac{R_{ab}(x') x^a x^b}{60} \right). \quad (64)$$

The second term vanishes in general and so does the third term when $R_{ab}(x') \propto g_{ab}(x')$ upto this order, and we recover (23). Thus, for sprinklings into a RNN with $R_{ab}(x') \propto g_{ab}(x')$ to this order, the continuum limit of the mean of (30) is approximately the correct value for the Green function of the conformally coupled massless field.

Defining

$$\mathcal{K}^{(4)}(a, b)(x, x') \equiv \sum_{k=0}^{\infty} a^{k+1} b^k L_k(x, x'), \quad (65)$$

we propose that this is the appropriate causal set Green function for the massive field and arbitrary coupling ξ in an RNN with $R_{ab}(x') \propto g_{ab}(x')$ to this order, for $a = \frac{1}{2\pi} \sqrt{\frac{\rho}{6}}$ and $b = -\frac{m^2 + (\xi - \frac{1}{6})R}{\rho}$.

We are unable to verify this directly as we lack knowledge about the mean of \mathbf{L}_k , the number of k -paths for $k \geq 1$, even in a RNN.

3.2.2 $d = 4$ de Sitter and anti de Sitter

In $d = 4$ for conformally flat spacetimes $g_{ab} = \Omega^2(x) \eta_{ab}$ the conformally coupled massless Green function is related to that in \mathbb{M}^4 by

$$G_{0, \xi_\epsilon}(x, x') = \Omega^{-1}(x) G_0^F(x, x') \Omega^{-1}(x'), \quad (66)$$

where $\xi_c = \frac{1}{6}$ and $G_0^F(x, x')$ denotes the retarded massless Green function in \mathbb{M}^4 . When g_{ab} in addition has constant scalar curvature the massive Green function for arbitrary ξ can be obtained from $G_{0, \xi_c}(x, x')$ using Eqn (40).

An example is the conformally flat patch of de Sitter spacetime

$$ds^2 = \frac{1}{(1 + Hx_0)^2} \left(-dx_0^2 + \sum_{i=1}^3 dx_i^2 \right), \quad (67)$$

where x_0 is the conformal time ($-\frac{1}{H} < x_0 < \infty$) and $H = \sqrt{\frac{\Lambda}{3}}$ with Λ the cosmological constant. The conformally coupled massless retarded Green function is

$$G_{0, \xi_c}(x, x') = \frac{1}{2\pi} \theta(t - t') \delta(\tau^2(x, x')) (1 + Hx_0)(1 + Hx'_0). \quad (68)$$

Since de Sitter is homogeneous, one can choose x' to lie at the convenient location $x' = (0, \vec{0})$ so that

$$G_{0, \xi_c}(x, x') = \frac{1}{2\pi} \theta(x_0) \delta(\tau^2(x, x')) (1 + Hx_0). \quad (69)$$

Taking our cue from the RNN calculation, we look to the link matrix $L_0(x, x')$ whose expectation value is given by Eqn (26). Taking $x' = (0, \vec{0})$, in the limit

$$\lim_{\rho \rightarrow \infty} \sqrt{\frac{\rho}{\pi}} \langle \mathbf{L}_0(x, x') \rangle = \theta(x_0) \theta(\tau^2(x, x')) \delta(\sqrt{V(x, x')}). \quad (70)$$

In order to evaluate this expression we need to find $V(x, x')$. In [14] this volume was calculated for a large interval when $\vec{x} = \vec{x}'$. However, it is the small volume limit that is relevant to our present calculation. When x lies in an RNN about x' , the calculation in the previous section suffices. However, we also need to consider intervals of small volume that lie outside of the RNN. These “long-skinny” intervals hug the future light cone of x' and it is this contribution to Eqn (70) that we will now consider.

In the following light cone coordinates

$$u = \frac{1}{2}(x_0 - x_3), v = \frac{1}{2}(x_0 + x_3), \quad (71)$$

let $u(x) = \epsilon$, $v(x) = L$, with $\alpha^2 \equiv \frac{\epsilon}{L} \ll 1$. Since there is a spatial rotational symmetry in de Sitter, we can also take $x_1 = x_2 = 0$. In order to simplify the calculation of $V(x, x')$, we perform a boost about x' in the $x_0 - x_3$ plane about x' so that $\tilde{x} = (\tilde{x}_0, \vec{0})$. The boost parameter is then $\beta = \frac{x_3}{x_0} \approx 1 - 2\alpha$. In these coordinates the conformal factor at a point $y = (y_0, \vec{y})$ is

$$\tilde{\Omega}^2(\tilde{y}) \approx \frac{1}{(1 + A(\tilde{y}_0 + \tilde{y}_3))^2} \quad (72)$$

where $A = \frac{1}{2}H\alpha$. Further transforming to cylindrical coordinates $(\tilde{y}_1, \tilde{y}_2, \tilde{y}_3) \rightarrow (r, \phi, \tilde{y}_3)$ we can split $V(x, x')$ into two multiple integrals

$$V_I(x, x') = \int_0^{-\frac{\tau}{2}} d\tilde{y}_0 \int_{-\tilde{y}_0}^{\tilde{y}_0} d\tilde{y}_3 \int_0^{\sqrt{\tilde{y}_0^2 - \tilde{y}_3^2}} r dr \int_0^{2\pi} d\phi \left(1 + A(\tilde{y}_0 + \tilde{y}_3)\right)^{-4} \quad (73)$$

$$V_{II}(x, x') = \int_{\frac{\tau}{2}}^{\tau} d\tilde{y}_0 \int_{-\tau + \tilde{y}_0}^{\tau - \tilde{y}_0} d\tilde{y}_3 \int_0^{\sqrt{(\tau - \tilde{y}_0)^2 - \tilde{y}_3^2}} r dr \int_0^{2\pi} d\phi \left(1 + A(\tilde{y}_0 + \tilde{y}_3)\right)^{-4} \quad (74)$$

with $V(x, x') = V_I(x, x') + V_{II}(x, x')$. Evaluating these expressions using $\tau^2 = 4L\epsilon$ we find that

$$\sqrt{V(x, x')} = \frac{1}{2} \sqrt{\frac{\pi}{6}} \frac{\tau^2}{(1 + A\tau)} \approx \frac{1}{2} \sqrt{\frac{\pi}{6}} \left(\frac{4L\epsilon}{1 + HL} \right), \quad (75)$$

which substituted into Eqn (70) gives

$$\lim_{\rho \rightarrow \infty} \sqrt{\frac{\rho}{\pi}} \langle \mathbf{L}_0(x, x') \rangle = \theta(t - t') \theta(\tau^2(x, x')) \sqrt{\frac{6}{\pi}} (1 + HL) \delta(4L\epsilon). \quad (76)$$

In the small α limit the conformally coupled de Sitter Green function is

$$G_{0, \xi_c}(x, x') \approx \frac{1}{2\pi} (1 + HL) \theta(x_0) \delta(4L\epsilon) \quad (77)$$

and hence

$$\lim_{\rho \rightarrow \infty} \frac{1}{2\pi} \sqrt{\frac{\rho}{6}} \langle \mathbf{L}_0(x, x') \rangle = G_{0, \xi_c}(x, x'). \quad (78)$$

As in the RNN, defining

$$\mathcal{K}^{(4)}(a, b)(x, x') \equiv \sum_{k=0}^{\infty} a^{k+1} b^k L_k(x, x'), \quad (79)$$

we propose that this is the appropriate causal set Green function for the massive field and arbitrary coupling ξ in de Sitter spacetime for $a = \frac{1}{2\pi} \sqrt{\frac{\rho}{6}}$ and $b = -\frac{m^2 + (\xi - \frac{1}{6})R}{\rho}$.

Although our calculation is restricted to the conformally flat patch of de Sitter spacetime, the result applies to global de Sitter, for the following reason. Let $x' \prec x$ in (global) de Sitter spacetime. Consider a Lorentz transformation about x' in the 5-dimensional Minkowski spacetime in which the hyperboloid that is de Sitter spacetime is embedded, which brings $\vec{x} = \vec{x}'$. This transformation preserves the hyperboloid. One can then choose the conformally flat patch of de Sitter with origin \vec{x}' , and use the above construction. When x, x' are not causally related, the Green functions vanish in both cases. Thus the Green function for global de Sitter is retarded if the conformally flat Green function is, and both satisfy the same equations, because there is no “wrap-around” in de Sitter.

The causal set Green function we propose is well defined on a sprinkling into global de Sitter. Moreover, as we have shown its continuum limit matches that of the Green function into the

conformally flat patch and thence from the above discussion, also the Green function of global de Sitter spacetime.

In anti de Sitter (adS) spacetime there exist pairs of events $x' \prec x$ such that $\tau(x, x')$ is finite, but $V(x, x')$ is infinite. While it is possible to obtain a Poisson sprinkling into such a spacetime, the resulting poset is not locally finite and hence not strictly a causal set. Such an interval is moreover not globally hyperbolic and hence falls outside the scope of our analysis. However, the interior of a conformally flat patch of adS (the so-called half-space) is globally hyperbolic and moreover, $V(x, x')$ is finite for every $x' \prec x$ in this region. Hence this patch of adS has a causal set description.

In the conformally flat patch the adS metric takes the form

$$ds^2 = \frac{1}{(1 + Hx_3)^2} \left(-dx_0^2 + \sum_{i=1}^3 dx_i^2 \right), \quad (80)$$

where we have off set the coordinates $x_3 \rightarrow x_3 + \frac{1}{H}$ in order to connect with the de Sitter calculation. Again choosing $x' = (0, \vec{0})$, we can write the massless Green function as

$$G_{0, \xi_c}(x, x') = \frac{1}{2\pi} \theta(x_0) \delta(\tau^2(x, x')) (1 + Hx_3). \quad (81)$$

In the boosted coordinates, upto order α^2 , the conformal factor

$$\Omega^2(y) = \frac{1}{(1 + Hy_3)^2} \approx \frac{1}{(1 + A(\tilde{y}_0 + \tilde{y}_3))^2} \quad (82)$$

and is identical to that of de Sitter in the calculation above. Moreover, to this order, $(1 + Hx_3) = (1 + H(L - \epsilon)) \approx (1 + HL)$, so that $\sqrt{V(x, x')}$ is given by Eqn (75). The same argument can then be carried through to show that the massive causal set Green function for arbitrary ξ in the conformally flat patch of de Sitter is given by Eqn (79).

We have thus proved *exact* results in de Sitter spacetime and in a conformally flat patch of anti de Sitter spacetime, namely that the mean of the causal set retarded Green function

$$\mathbf{K}_0(x, x') = \frac{1}{2\pi} \sqrt{\frac{\rho}{6}} \langle \mathbf{L}_0(x, x') \rangle \quad (83)$$

is equal to the continuum massless conformally coupled Green function in the limit $\rho \rightarrow \infty$. In addition, we make the proposal that the limit of the mean of $\mathcal{K}^{(4)}(a, b)(x, x')$ with the appropriate a and b is the continuum massive Green function for arbitrary conformal coupling ξ .

4 Discussion

We have demonstrated that Johnston's hop-stop model for a Green function on a causal set can be generalised whenever an identification can be made of the massless retarded Green function.

As a final illustration, we make a proposal for the causal set Green function in $d = 3$ Minkowski spacetime. In continuum flat spacetime in 3 dimensions the massless scalar propagator is

$$G_0^{(3)}(x, x') = \theta(t - t')\theta(\tau^2) \frac{1}{2\pi\tau(x, x')}, \quad (84)$$

where for now we ignore the singular behaviour at $\tau(x, x') = 0$. The causal set counterpart of the proper time $\tau(x, x')$ in ${}^d\mathbb{M}$ was given by Brightwell and Gregory [16] to be proportional to the *length* $l(x, x')$ of the longest chain (LLC) from x' to x , where length of a k -chain is taken to be $k + 1$. Explicitly

$$\lim_{\rho \rightarrow \infty} \langle \mathbf{1}(x, x') \rangle (\rho V(x, x'))^{-1/d} = m_d \quad (85)$$

where m_d is a dimension dependent constant bounded by

$$1.77 \leq \frac{2^{1-\frac{1}{d}}}{\Gamma(1+\frac{1}{d})} \leq m_d \leq \frac{2^{1-\frac{1}{d}} e (\Gamma(1+d))^{\frac{1}{d}}}{d} \leq 2.62. \quad (86)$$

In ${}^d\mathbb{M}$, $\rho V(x, x') = \zeta_d \tau^d(x, x')$ with ζ_d a dimension dependent constant, so that

$$\lim_{\rho \rightarrow \infty} \rho^{-\frac{1}{d}} \langle \mathbf{1}(x, x') \rangle = \kappa_d \tau(x, x') \quad (87)$$

where $\kappa_d \equiv m_d (\zeta_d)^{1/d}$. This *suggests* that the $d = 3$ massless Green function on C is

$$K_0(x, x') \equiv a H_0(x, x'). \quad (88)$$

where

$$H_0(x, x') \equiv \begin{cases} \frac{1}{l(x, x')} & \text{if } x' \prec x \\ 0 & \text{otherwise.} \end{cases} \quad (89)$$

This will give us the desired $d = 3$ Green function if it were also true that

$$\lim_{\rho \rightarrow \infty} \left\langle \frac{1}{l(x, x')} \right\rangle \rho^{\frac{1}{3}} = \frac{1}{\kappa_3 \tau(x, x')} \quad (90)$$

then comparison with Eqn (84) gives $a = \rho^{1/3} \frac{\kappa_3}{2\pi} = (\frac{\rho\pi}{12})^{1/3} \frac{m_3}{2\pi}$.

While we do not have an analytical proof of Eqn (90), simulations shown in Appendix B demonstrate that for large ρ , $\langle \frac{1}{l(x, x')} \rangle \rightarrow \frac{1}{\langle l(x, x') \rangle}$ and hence Eqn (90) is indeed a good approximation.

In order to extend this to the massive case, we need to ask what the analogue of the convolution in (15) is. Because of the non-trivial weight $\frac{1}{l(x, x')}$, we cannot simply count chains

to get C_k . The convolution

$$\langle \mathbf{H}_0 \rangle * \langle \mathbf{H}_0 \rangle = \rho \int d^3 x_1 \langle \mathbf{H}_0(x, x_1) \rangle \langle \mathbf{H}_0(x_1, x') \rangle = \langle \mathbf{H}_1(x, x') \rangle \quad (91)$$

where

$$H_1(x, x') = \sum_{x_1} H_0(x, x_1) H_0(x_1, x') = \sum_{x_1} \frac{1}{l(x, x_1)} C_0(x, x_1) \frac{1}{l(x_1, x')} C_0(x_1, x'). \quad (92)$$

counts instead the number of 1-chains weighted by the inverse of the length of the longest possible chain in C between each successive pair of joints in the given chain. As in $d = 2$ the trajectories are chains, but the $H_k(x, x')$ are not obtained by merely counting chains; each k -chain is weighted by the inverse of the length of the longest possible chain C between each pair of joints in the given chain.

Again defining

$$\mathcal{K}^{(3)}(a, b)(x, x') \equiv \sum_{k=0}^{\infty} a^{k+1} b^k H_k(x, x'), \quad (93)$$

we propose that this is the appropriate causal set Green function for the massive field for $a = (\frac{\rho\pi}{12})^{1/3} \frac{m_3}{2\pi}$ and $b = -\frac{m^2}{\rho}$.

In [4] a proposal for the $d=3$ Green function was made using the relationship between $\tau(x, x')$ and the volume $V(x, x')$, $\tau(x, x') \propto V(x, x')^{\frac{1}{3}}$. Our proposal uses instead the causal set analogue of $\tau(x, x')$ directly. In the large ρ limit, one would expect both proposals to give the same result.

In principle, the causal set Green functions in $d > 4$ can also be obtained. Massless propagators in the continuum are derivatives of either $\frac{1}{\tau}$ or $\delta(\tau^2)$ depending on whether d is odd or even. Since derivatives of $\delta(\tau^2)$ of any order can always be written as products of $\delta(\tau^2)$ and $\frac{1}{\tau}$, the knowledge of the causal set analogues of these two quantities with appropriate weights suffices to write down the discrete propagator. We leave this to future work.

Another aspect we have ignored in this work are the causal set induced corrections to the retarded Green functions. Given that causal set theory posits a fundamental discreteness, the $\rho \rightarrow \infty$ limit is only a mathematical convenience. Indeed it is the large ρ corrections to the continuum Green function which are phenomenologically interesting. This has been explored in [17] for cases of $d = 2$ and 4 Minkowski spacetime. Also, while our analysis has focused on the mean of the causal set Green function, we have not analysed the fluctuations. We hope to be able to address these issues in the future.

5 Acknowledgements

This work was supported in part under an agreement with Theiss Research and funded by a grant from the FQXI Fund on the basis of proposal FQXi-RFP3-1346 to the Foundational Questions Institute. FD's work is supported in part by STFC grant ST/L00044X/1. Simulations were performed using the `CausalSets` toolkit [18] within the `Cactus` high performance computing framework [19]. NX would like to thank David Rideout and Simran Singh for helpful discussions on `Cactus`.

References

- [1] L. Bombelli, J. Lee, D. Meyer and R. Sorkin, *Phys. Rev. Lett.* **59**, 521 (1987). doi:10.1103/PhysRevLett.59.521
- [2] A. R. Daughton, UMI-94-01667.
- [3] S. Johnston, *Class. Quant. Grav.* **25**, 202001 (2008) doi:10.1088/0264-9381/25/20/202001 [arXiv:0806.3083 [hep-th]].
- [4] S. P. Johnston, arXiv:1010.5514 [hep-th].
- [5] D. M. T. Benincasa, F. Dowker and B. Schmitzer, *Class. Quant. Grav.* **28**, 105018 (2011) doi:10.1088/0264-9381/28/10/105018 [arXiv:1011.5191 [gr-qc]].
- [6] S. Aslanbeigi, M. Saravani and R. D. Sorkin, *JHEP* **1406**, 024 (2014) doi:10.1007/JHEP06(2014)024 [arXiv:1403.1622 [hep-th]].
- [7] S. Johnston, *Phys. Rev. Lett.* **103**, 180401 (2009) doi:10.1103/PhysRevLett.103.180401 [arXiv:0909.0944 [hep-th]].
- [8] N. Afshordi, S. Aslanbeigi and R. D. Sorkin, *JHEP* **1208**, 137 (2012) doi:10.1007/JHEP08(2012)137 [arXiv:1205.1296 [hep-th]].
- [9] R. D. Sorkin, *J. Phys. Conf. Ser.* **306**, 012017 (2011) doi:10.1088/1742-6596/306/1/012017 [arXiv:1107.0698 [gr-qc]].
- [10] T. S. Bunch and L. Parker, *Phys. Rev. D* **20**, 2499 (1979). doi:10.1103/PhysRevD.20.2499
- [11] M. Roy, D. Sinha and S. Surya, *Phys. Rev. D* **87**, no. 4, 044046 (2013) doi:10.1103/PhysRevD.87.044046 [arXiv:1212.0631 [gr-qc]].

- [12] D. M. T. Benincasa and F. Dowker, Phys. Rev. Lett. **104**, 181301 (2010) doi:10.1103/PhysRevLett.104.181301 [arXiv:1001.2725 [gr-qc]].
- [13] J. Myrheim, CERN-TH-2538.
- [14] G. W. Gibbons and S. N. Solodukhin, Phys. Lett. B **649**, 317 (2007) doi:10.1016/j.physletb.2007.03.068 [hep-th/0703098].
- [15] S. Khetrpal and S. Surya, Class. Quant. Grav. **30**, 065005 (2013) doi:10.1088/0264-9381/30/6/065005 [arXiv:1212.0629 [gr-qc]].
- [16] G. Brightwell and R. Gregory, Phys. Rev. Lett. **66**, 260 (1991). doi:10.1103/PhysRevLett.66.260
- [17] S. Johnston, Class. Quant. Grav. **32**, no. 19, 195020 (2015) doi:10.1088/0264-9381/32/19/195020 [arXiv:1411.2614 [hep-th]].
- [18] G. Allen and T. Goodale and F. Löffler and D. Rideout and E. Schnetter and E. Seidel, “Component Specification in the Cactus Framework: The Cactus Configuration Language” in *Workshop on Component-Based High Performance Computing – CBHPC 2010*
- [19] T. Goodale, G. Allen, G. Lanfermann, J. Massó, T. Radke, E. Seidel, and J. Shalf, “The Cactus Framework and Toolkit: Design and Applications” in *Vector and Parallel Processing – VECPAR 2002, 5th International Conference*, Springer, pp. 197–227.
- [20] M. J. Lighthill, *An Introduction to Fourier Analysis and Generalised Functions*, Cambridge University Press (1958).

6 Appendix A

Define the function

$$h_n(\rho, z) \equiv \sqrt{\rho}(\pi c \rho z^2)^n e^{-\pi c \rho z^2}, \quad (94)$$

where $n \geq 0$. We now show that

$$\lim_{\rho \rightarrow \infty} h_n(\rho, z) = \frac{\Gamma(n + 1/2)}{\sqrt{\pi c}} \delta(z). \quad (95)$$

First, we evaluate the integral

$$\begin{aligned} \int_{-\infty}^{\infty} dz h_n(\rho, z) &= 2\sqrt{\rho} \int_0^{\infty} dz (\pi c \rho z^2)^n e^{-\pi c \rho z^2} \\ &= \frac{1}{\sqrt{\pi c}} \int_0^{\infty} dt (t)^{n-1/2} e^{-t} \\ &= \frac{\Gamma(n + 1/2)}{\sqrt{\pi c}}, \end{aligned} \quad (96)$$

which is independent of ρ . Next, we integrate $h_n(\rho, z)$ with an analytic test function and take the limit $\rho \rightarrow \infty$. If $f(z)$ is odd, the integral vanishes (this also happens with the delta function) and we can restrict to even analytic functions

$$f(z) = \sum_{k=0}^{\infty} a_k z^{2k}. \quad (97)$$

For this,

$$\begin{aligned} \lim_{\rho \rightarrow \infty} \int_{-\infty}^{\infty} dz f(z) h_n(\rho, z) &= \lim_{\rho \rightarrow \infty} \sum_{k=0}^{\infty} a_k \int_{-\infty}^{\infty} dz z^{2k} h_n(\rho, z) \\ &= \lim_{\rho \rightarrow \infty} 2 \sum_{k=0}^{\infty} a_k \int_0^{\infty} dz z^{2k} \sqrt{\rho} (\pi c \rho z^2)^n e^{-\pi c \rho z^2} \\ &= \lim_{\rho \rightarrow \infty} 2 \sum_{k=0}^{\infty} a_k \frac{\sqrt{\rho}}{(\pi c \rho)^k} \int_0^{\infty} dz (\pi c \rho z^2)^{n+k} e^{-\pi c \rho z^2} \\ &= \lim_{\rho \rightarrow \infty} \sum_{k=0}^{\infty} a_k \frac{\Gamma(n+k+1/2)}{\sqrt{\pi c} (\pi c \rho)^k} \\ &= a_0 \frac{\Gamma(n+1/2)}{\sqrt{\pi c}} = \frac{\Gamma(n+1/2)}{\sqrt{\pi c}} f(0). \end{aligned}$$

Noting that $n = 0$ is the usual Gaussian integral, and that the behaviour with test functions is one way to define a delta function [20], this proves Eqn (95).

7 Appendix B

Here we present simulations that provide support for Eqn (90) for large ρ . Starting with Eqn (90) in $d = 3$ we see that

$$\lim_{N \rightarrow \infty} \left\langle \frac{1}{l(x, x')} \right\rangle \left(\frac{N}{V(x, x')} \right)^{\frac{1}{3}} = \frac{1}{m_3 \zeta_3^{1/3} \tau(x, x')} \quad (98)$$

where we have used $\rho = \frac{N}{V} = \frac{N}{\zeta_3 \tau^3}$ and $\zeta_3 = \frac{\pi}{12}$. Since the volume $V(x, x')$ is fixed, the limit $\rho \rightarrow \infty$ is the same as $N \rightarrow \infty$ and hence this simplifies to

$$\lim_{N \rightarrow \infty} \left\langle \frac{1}{l(x, x')} \right\rangle = \frac{1}{m_3 N^{1/3}} \quad (99)$$

Using Eqn (86) we see that

$$b_l := \frac{1}{1.77 N^{1/3}} \leq \lim_{N \rightarrow \infty} \left\langle \frac{1}{l(x, x')} \right\rangle \leq \frac{1}{2.62 N^{1/3}} =: b_u \quad (100)$$

where we have defined b_l and b_u as the lower and upper bounds respectively.

We calculate $\langle \frac{1}{l(x,x')} \rangle$ and $\frac{1}{\langle l(x,x') \rangle}$ for sprinklings into a causal diamond in ${}^3\mathbb{M}$, for N values ranging from 100 to 50000 in steps of 100. For each N value we perform over 50 trials from which the averages are calculated. Our results are shown in Figs (2a)-(2e).

In Fig (2a) we see that $\langle \frac{1}{l(x,x')} \rangle$ is well within the bounds b_l and b_u . In Fig (2b) we show the percentage errors defined by

$$\delta_l := \frac{1}{b_l} \left(\left\langle \frac{1}{l(x,x')} \right\rangle - b_l \right) \times 100 \quad \text{and} \quad \delta_u := \frac{1}{b_u} \left(\left\langle \frac{1}{l(x,x')} \right\rangle - b_u \right) \times 100$$

with respect to the lower and upper bounds. While there is a convergence for large N the error does not go to zero for either of the bounds.

It is also useful to compare $\langle \frac{1}{l(x,x')} \rangle$ to $\frac{1}{\langle l(x,x') \rangle}$ since it is the theoretical bound on the latter which we are using. As shown in (Fig (2c)) we find an almost perfect matching of $\langle \frac{1}{l(x,x')} \rangle$ with $\frac{1}{\langle l(x,x') \rangle}$ even at relatively small N values. We plot the percentage error in Fig (2d) where

$$\Delta := \left(\left\langle \frac{1}{l(x,x')} \right\rangle \right)^{-1} \left(\left\langle \frac{1}{l(x,x')} \right\rangle - \frac{1}{\langle l(x,x') \rangle} \right) \times 100$$

which is already very small for $N \sim 200$ and dies down further as N grows.

Using the ‘‘FindFit’’ function in Mathematica we find that the best fit value for m_3 is in fact 1.854 for the range of N that we have considered. As can be seen in Figure (2e) the errors for this fit are very small.

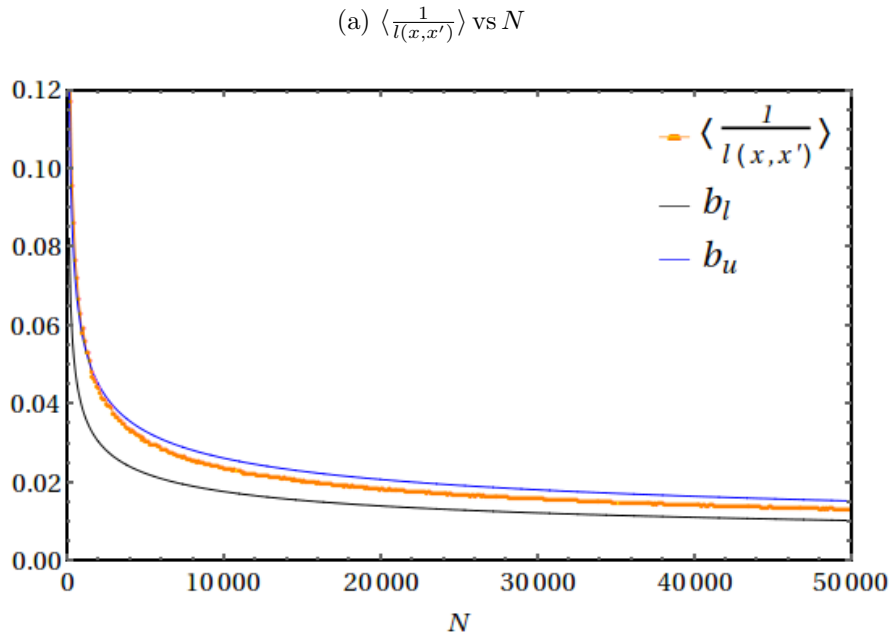
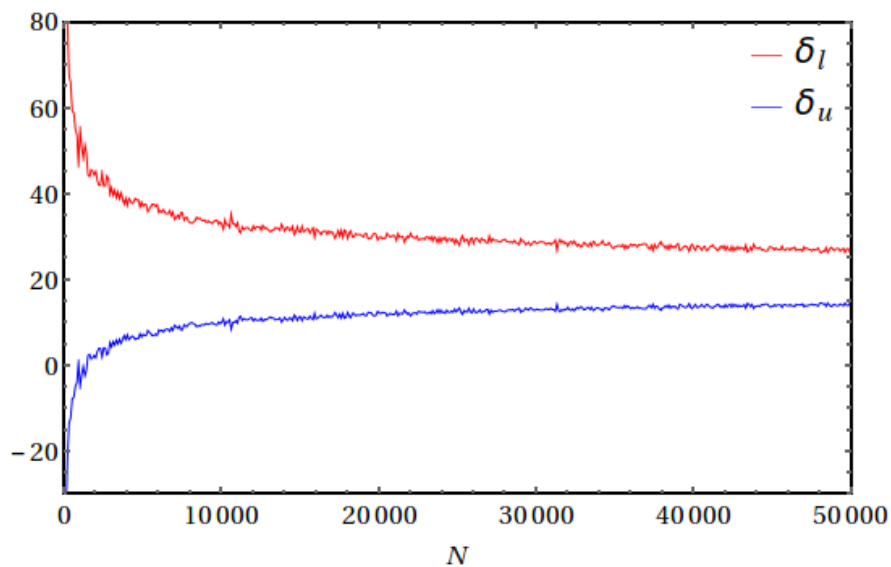


Figure 2: Fig (a) shows a comparison of $\langle \frac{1}{l(x,x')} \rangle$ as a function of N , with the conjectured upper and lower bounds.

(b) Errors in $\langle \frac{1}{l(x,x')} \rangle$ with respect to b_u, b_l



(c) Comparison of $\langle \frac{1}{l(x,x')} \rangle$ and $\frac{1}{\langle l(x,x') \rangle}$

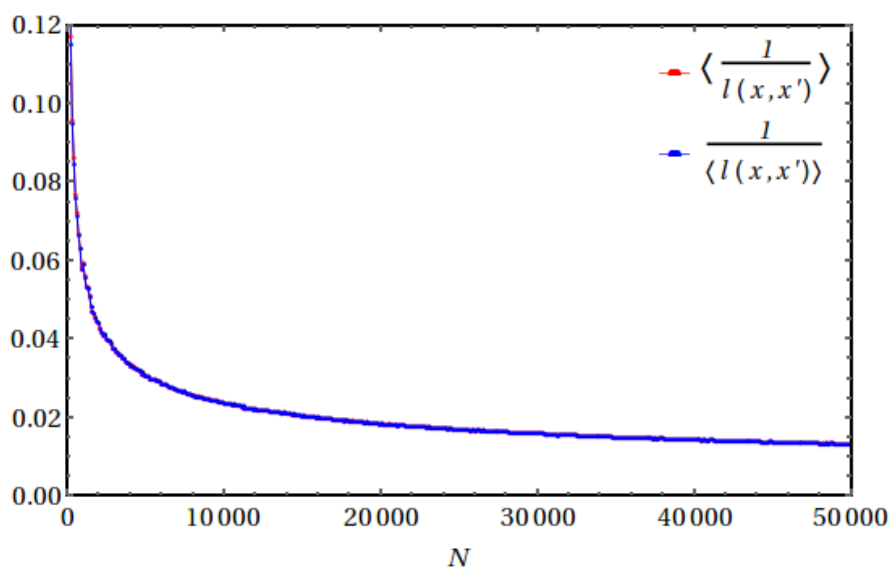
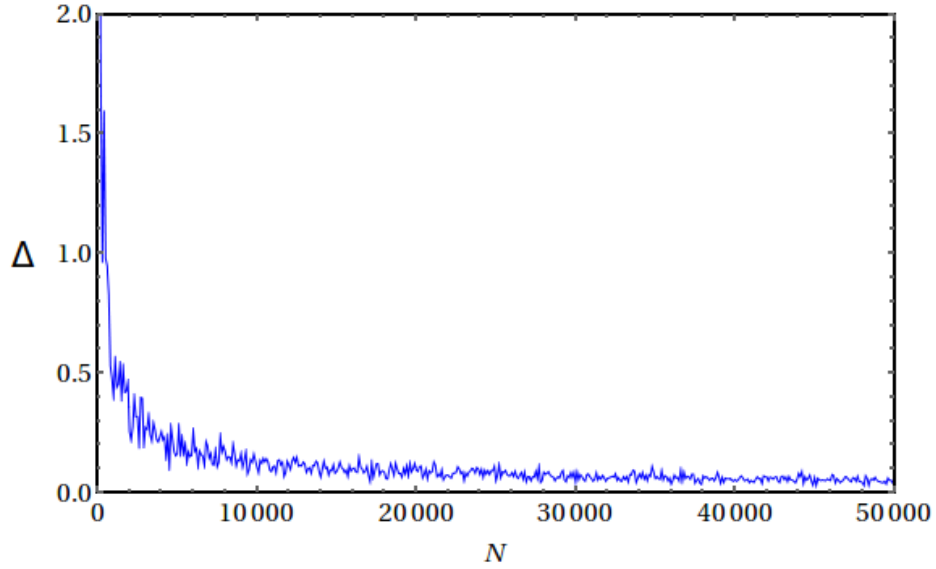


Figure 2: Fig (b) gives the percentage error estimation with respect to these bounds. Fig (c) shows $\langle \frac{1}{l(x,x')} \rangle$ and $\frac{1}{\langle l(x,x') \rangle}$ vs N

(d) Error in $\frac{1}{\langle l(x,x') \rangle}$ with respect to $\langle \frac{1}{l(x,x')} \rangle$



(e) Error in $\langle \frac{1}{l(x,x')} \rangle$ with respect to the Best Fit

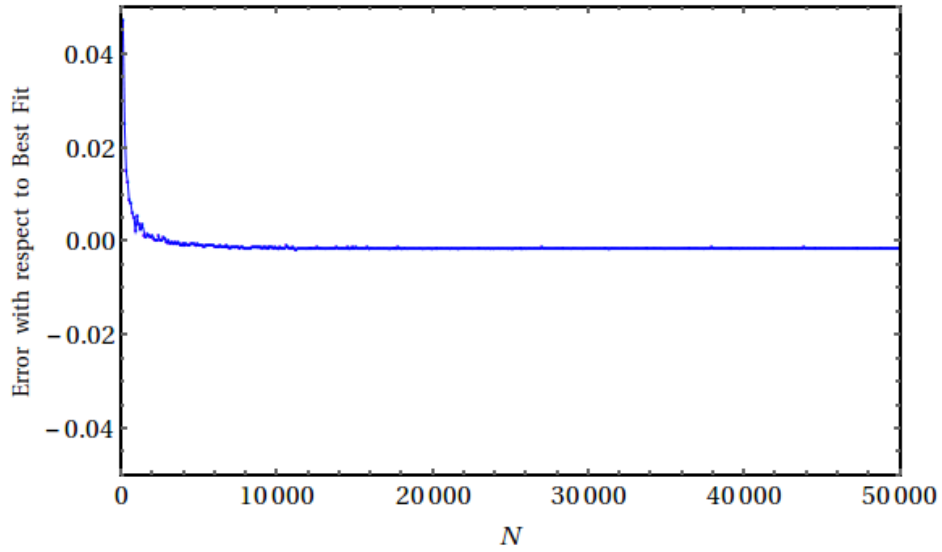


Figure 2: Fig (d) shows the percentage error between $\frac{1}{\langle l(x,x') \rangle}$ and $\langle \frac{1}{l(x,x')} \rangle$. This rapidly goes to zero as N increases. Fig (e) shows the difference between $\langle \frac{1}{l(x,x')} \rangle$ and the best fit with $m_3 = 1.854$, this too goes to zero rapidly.